Global Change Biology (2011) 1–12, doi: 10.1111/j.1365-2486.2011.02481.x

A test of a field-based ^{15}N–nitrous oxide pool dilution technique to measure gross N_2O production in soil

WENDY H. YANG*,A, YIT ARN TEH† and WHENDEE L. SILVER*

*Ecosystem Sciences Division, Department of Environmental Science, Policy, and Management, University of California, 137 Mulford Hall #3114, Berkeley, CA, 94720, USA, †Environmental Change Research Group, School of Geography and Geosciences, University of St. Andrews, St. Andrews, KY169 AL, UK

Abstract

Soils are both a major source and sink of nitrous oxide (N_2O), but the proportion of soil N_2O production released to the atmosphere (termed the N_2O yield) is poorly constrained due to the difficulty in measuring gross N_2O production. The quantification of gross N_2O fluxes would greatly improve our ability to predict N_2O dynamics across the soil-atmosphere interface. We report a new approach, the $^{15}N_2O$ pool dilution technique, to measure rates of gross N_2O production and consumption under laboratory and field conditions. In the laboratory, gross N_2O production and consumption compared well between the $^{15}N_2O$ pool dilution and acetylene inhibition methods whereas the $^{15}NO_3^-$ tracer method measured significantly higher rates. In the field, N_2O emissions were not significantly affected by increasing chamber headspace concentrations up to 100 ppb $^{15}N_2O$. The pool dilution model estimates of $^{14}N_2O$ and $^{15}N_2O$ concentrations as well as net N_2O fluxes fit observed data very well, suggesting that the technique yielded robust estimates of gross N_2O production. Estimated gross N_2O consumption rates were underestimated relative to rates calculated as the difference between gross and net N_2O production rates, possibly due to heterogeneous and/or inadequate tracer diffusion to deeper layers in the soil profile. Gross N_2O production rates were high, averaging 8.4 ± 3.2 mg N m^{-2} day^{-1}, and were most strongly correlated to mineral nitrogen concentrations and denitrifying enzyme activity (R^2 = 0.73). Gross N_2O production rates varied spatially, with the highest rates in soils with the best drainage and the highest mineral N availability. Estimated and calculated N_2O consumption rates constrained the average N_2O yield from 0.70 to 0.84. Our results demonstrate that the $^{15}N_2O$ pool dilution technique can provide well-constrained estimates of N_2O yields and field rates of gross N_2O production correlated to soil characteristics, improving our understanding of terrestrial N_2O dynamics.

Keywords: denitrification, N_2O yield, nitrous oxide, pool dilution, Sacramento–San Joaquin Delta

Received 7 April 2011 and accepted 23 May 2011

Introduction

Nitrous oxide (N_2O) is a potent greenhouse gas and catalyst for stratospheric ozone depletion that has been accumulating in the atmosphere since the Industrial Revolution (Prather *et al*., 1995). Nitrous oxide emissions from natural and agricultural soils represent over half of global N_2O emissions (Stein & Yung, 2003). Nitrification and denitrification, both dominantly microbial processes, are primarily responsible for N_2O production in soil. Denitrifiers can also consume N_2O to dinitrogen (N_2), an inert gas that constitutes 78% of Earth's atmosphere. Soil N_2 production is very difficult to detect against the high background atmospheric N_2 concentration, and methods to indirectly measure soil N_2 emissions have well-recognized limitations (Groffman *et al*., 2006). While considerable effort has been directed at measuring or estimating N_2 emissions from soils, less attention has been paid to directly measuring gross (i.e. total) N_2O production. The inability to accurately quantify soil N_2 emissions or gross N_2O production contributes to uncertainty in the amount of nitrogen (N) denitrified in terrestrial ecosystems (Kulkarni *et al*., 2008). This leaves ecosystem N budgets poorly constrained and also limits our ability to predict the effects of global change and human activities on future ecosystem N budgets and soil N_2O emissions (Boyer *et al*., 2006).

Theory suggests that the proportion of gross N_2O production that results in N_2O emissions (termed the N_2O yield) should follow predictable patterns, varying as a function of substrate availability and micro-environmental conditions. For example, high soil nitrate (NO_3^-) availability inhibits N_2O consumption (Blackmer & Bremner, 1978; Firestone *et al*., 1979, 1980; Weier *et al*., 1993), leading to higher N_2O yields in N rich ecosystems. However, a recent review reported that N_2O

Correspondence: Wendy H. Yang, tel. +1 510 643 3963, fax +1 510 643 5098, e-mail: wendy_yang@berkeley.edu

GCB 2481 B | Dispatch: 27.6.11 | Journal: GCB | CE: Anusha | Journal Name | Manuscript No. | Author Received: | No. of pages: 13 | PE: Eswari

yields for agricultural soils span the entire possible range from 0 to 1 (Schlesinger, 2009). This broad range may reflect uncertainties associated with the existing methods for measuring gross soil N_2O production rates that often require soil to be incubated in the laboratory (Groffman *et al.*, 2006). Both nitrification and denitrification are redox sensitive processes and as such, changes in oxygen (O_2) availability can affect N_2O yields (Firestone *et al.*, 1979, 1980; Goreau *et al.*, 1980; Bollmann & Conrad, 1998). *In situ* measurements of gross soil N_2O production could help constrain N_2O yields for terrestrial ecosystems.

The stable isotope pool dilution technique has been widely employed to study gross N mineralization and nitrification in soils (Kirkham & Bartholomew, 1954; Booth *et al.*, 2005) and can also be used to measure simultaneous production and consumption of trace gases in soil. The trace gas approach is based on the addition of a heavy stable isotope tracer to the product pool in the headspace of a closed laboratory incubation chamber containing soil or in a field flux chamber inserted into the soil surface. Gross process rates can be estimated from concurrent isotopic dilution of the isotopically labeled pool by production at natural abundance isotopic composition and the disappearance of the isotopic tracer by biological consumption. For trace gas pool dilution, isotope tracer loss due to physical processes (i.e. diffusion and advection) is accounted for using a conservative tracer such as sulfurhexafluoride (SF_6). This technique has been successfully used to measure simultaneous soil production and consumption of methane (von Fischer & Hedin, 2002) and methyl halides (Rhew *et al.*, 2003; Rhew & Abel, 2007) in the field and laboratory. The use of $^{15}N_2O$ as a tracer for N_2O consumption has been explored in a laboratory soil column (Clough *et al.*, 2006), in ground water (Clough *et al.*, 2007), and in estuarine waters (Punshon & Moore, 2004), but the $^{15}N_2O$ pool dilution technique has not been previously tested.

Here we report on the application of the pool dilution technique to surface flux measurements of gross N_2O production and consumption in soil. As opposed to methane and methyl halides, which are generally produced at depth in soil and consumed by oxidative processes at the soil surface, N_2O could be produced or consumed at the soil surface or at depth depending on environmental conditions. The steady state diffusion of N_2O from soil into a surface flux chamber integrates over time and space so that gross N_2O production rates estimated by pool dilution are valid regardless of where in the soil profile N_2O production occurs. This steady state assumption is likely valid for the short time period over which the measurement occurs.

In contrast to gross N_2O production, gross N_2O consumption rates may be overestimated by the pool dilution technique if $^{15}N_2O$ additions stimulate consumption or underestimated if the isotopic tracer does not diffuse to sites of consumption within the soil profile. Stimulation of consumption is a long standing problem with isotope dilution techniques (Davidson *et al.*, 1991; reviewed by Booth *et al.*, 2005), which are generally best suited for estimating gross production rates. With $^{15}N_2O$ pool dilution, however, underestimation of gross consumption rates may be more important, especially in compacted or wet soils in which tracer diffusion through the vadose zone is slow.

The potential for underestimation of N_2O consumption by the $^{15}N_2O$ pool dilution technique can be tested and constrained using several different approaches. First, diffusion modeling can be used to estimate isotope tracer penetration into the unsaturated soil profile (von Fischer *et al.*, 2009). Second, the distribution of denitrifying enzyme activity, a good index of denitrification potential (Smith & Tiedje, 1979), can be measured through the vadose zone. Biased distribution of the ^{15}N label by depth can impact gross N transformation rates estimated using the pool dilution technique, but this impact is limited when ^{15}N enrichment decreases with depth and gross N transformation rates also decrease with depth or are uniform throughout the soil profile (Davidson *et al.*, 1991). Third, assuming steady state N_2O dynamics during the relatively short measurement interval, N_2O consumption rates estimated by pool dilution can be compared with N_2O consumption rates calculated as the difference between gross N_2O production rates and observed net N_2O fluxes. This last approach can be used to quantitatively evaluate gross N_2O consumption rates measured by ^{15}N tracer loss as well as provide a second estimate to constrain gross N_2O consumption rates.

In this study, we tested the $^{15}N_2O$ pool dilution technique in a N-rich managed grassland. The objectives of this study were to: (i) evaluate the application of the pool dilution technique to N_2O dynamics, (ii) constrain the N_2O yield for this site, and (iii) examine the controls on gross N_2O production and consumption rates and the N_2O yield.

Methods

Trace gas pool dilution model

Gross N_2O production rates were determined using the modeling approach described by von Fischer & Hedin (2002) for gross methane production. The trace gas pool dilution model uses the following two equations (Eqns 1 and 2), with input variables of $[^{14}N_2O]_t$ and $[^{15}N_2O]_t$, the concentrations of $^{14}N_2O$

and $^{15}N_2O$ at time t; F_{14} and F_{15}, the $^{14}N_2O$ and $^{15}N_2O$ mole fractions of N_2O produced; k_{14} and k_{15}, the first-order rate constants for $^{14}N_2O$ and $^{15}N_2O$ reduction to N_2; k_L, the first-order rate constant for loss of the conservative tracer, SF_6. P, the gross N_2O production rate (mg N m^{-2} d^{-1}), is the unknown variable in each equation.

$$[^{14}N_2O] = \frac{F_{14} \times P}{k_{14}} - \left(\frac{F_{14} \times P}{k_{14}} - [^{14}N_2O]_0\right) \times \exp\{-k_{14} \times (t - t_0)\} \quad (1)$$

$$[^{15}N_2O] = \frac{F_{15} \times P}{k_{15} - k_L} - \left(\frac{F_{15} \times P}{k_{15} - k_L} - [^{15}N_2O]_0\right) \times \exp\{-(k_{15} + k_L) \times (t - t_0)\}. \quad (2)$$

The concentration of $^{15}N_2O$ ($[^{15}N_2O]_t$) is calculated as the product of N_2O concentration and ^{15}N–N_2O atom% excess assuming that the ^{15}N isotopic composition of background N_2O is the average tropospheric value of 6.72 per mil (relative to atmospheric N_2) or 0.3688 atom% (Kaiser *et al.*, 2003). $[^{14}N_2O]_t$ is calculated as the product of N_2O concentration and ^{14}N–N_2O atom% (i.e. 100 minus ^{15}N–N_2O atom%).

The mole fractions of $^{14}N_2O$ and $^{15}N_2O$ produced (F_{14} and F_{15}) were calculated assuming that the initial substrates were at natural abundance ^{15}N (0.3663 atom%). The average literature values for the fractionation factors associated with N_2O production are 0.9188 ± 0.0308 (mean ± SD) for nitrification (Table S1) and 0.9703 ± 0.0118 for denitrification (Table S2). Assuming that nitrification and denitrification contributed equally to N_2O production (i.e. averaging the mean fractionation factors for nitrification and denitrification), the isotopic composition of the N_2O produced is calculated to be 0.3431 atom% ^{15}N. We performed sensitivity analyses to evaluate the effect of variations in the assumed $^{14}N_2O$ and $^{15}N_2O$ mole fractions of N_2O produced on gross N_2O production and consumption rates estimated by the pool dilution model. We assumed relative contributions of nitrification and denitrification to N_2O production that ranged from all nitrification and no denitrification to all denitrification and no nitrification; the model output changed by <1% in response to the range of the $^{14}N_2O$ and $^{15}N_2O$ mole fractions of N_2O produced.

The first-order rate constant for $^{14}N_2O$ reduction to N_2 (k_{14}) is calculated from the fractionation factor (α) and the observed first-order rate constant for $^{15}N_2O$ reduction to N_2 (k_{15}) for each measurement using the definition, $\alpha = k_{15}/k_{14}$. The fractionation factor associated with N_2O reduction to N_2 is assumed to be the average literature value, 0.9924 ± 0.0036 (Table S3). Sensitivity analysis using the range of literature values (0.9860–0.9976) showed that the model output is not sensitive to the fractionation factor value, changing by <1% over the entire range.

The first-order exponential decay constant for observed $^{15}N_2O$ concentrations over time (k_{15}) represents biological and physical loss whereas k_L, the first-order exponential decay constant for SF_6 concentrations over time, represents only physical loss (i.e. diffusion and/or advection). Thus, the difference in the k-values is deduced to be the biological loss of $^{15}N_2O$ due to N_2O consumption to N_2 through denitrification. The use of SF_6 as a tracer for physical loss of N_2O is reasonable based on observations of similar loss rates for SF_6 and CFC-113 despite different molecular properties (Rhew *et al.*, 2003). Sulfurhexafluoride has been used as a conservative tracer to follow N_2O dynamics in soil (Clough *et al.*, 2006) and aquatic ecosystems (e.g. Addy *et al.*, 2002, 2005; Clough *et al.*, 2007). In the field, the tracer loss can be approximated as a first-order process based on observed loss rates (Fig. S1; Rhew & Abel, 2007). Nitrous oxide production and consumption also follow first-order kinetics (Vieten *et al.*, 2007, 2009).

We solved the trace gas pool dilution model iteratively for gross N_2O production rate, P; the initial concentrations of $^{14}N_2O$ and $^{15}N_2O$, $[^{14}N_2O]_0$ and $[^{15}N_2O]_0$; and k_{15}. The model seeks to minimize the error estimated by the following equation (Eqn 3), where $[^{14}N_2O]_{est}$ and $[^{15}N_2O]_{est}$ are the estimated $^{14}N_2O$ and $^{15}N_2O$ concentrations; $[^{14}N_2O]_{obs}$ and $[^{15}N_2O]_{obs}$ are the observed $^{14}N_2O$ and $^{15}N_2O$ concentrations; and p is the instrument precision. The instrument precision (expressed as standard deviation) is calculated by Gaussian error propagation from the standard deviation of all standards analyzed on the IRMS and GC on the days the relevant samples were analyzed (Zar, 1998). The model goodness of fit was evaluated by regressing $[^{14}N_2O]_{pred}$ against $[^{14}N_2O]_{obs}$; a slope of 1 for the regression line represents a good fit.

$$E = \sum\{([^{14}N_2O]_{est}(t) - [^{14}N_2O]_{obs}(t))^2\} \times p + \sum\{([^{15}N_2O]_{est}(t) - [^{15}N_2O]_{obs}(t))^2\} \times p. \quad (3)$$

Gross N_2O consumption rates can be determined using multiple approaches. First, it can be determined empirically from the losses of $^{15}N_2O$ and SF_6 from the chamber headspace over time. The measured gross N_2O consumption rate is calculated as the product of the biological N_2O loss rate (i.e. $k_{15} - k_L$) and the N_2O concentration of background field air. This approach will lead to underestimated N_2O consumption rates if gross N_2O production rates are high (see below). Second, the observed $^{15}N_2O$ loss rate (k_{15}) can be used as the initial value in the iterative pool dilution model that solves for k_{15} to best fit estimated $^{14}N_2O$ and $^{15}N_2O$ concentrations to observed $^{15}N_2O$ and $^{15}N_2O$ concentrations. With this approach, gross N_2O consumption rates are estimated by the pool dilution model. Third, the gross N_2O consumption rate can be calculated as the difference between the estimated gross N_2O production rate and measured net N_2O flux. Measured net N_2O fluxes are determined from the change in N_2O concentration in the chamber headspace over time.

The trace gas pool dilution model includes terms for the $^{14}N_2O$ and $^{15}N_2O$ mole fractions of N_2O produced and the fractionation that occurs during N_2O consumption, but these effects are not transmitted to k_{15} if it is fixed at the observed value. In situations in which gross N_2O production and consumption rates are very high, nontrivial increases in the amount of $^{15}N_2O$ in the chamber headspace can occur for two reasons. First, naturally occurring $^{15}N_2O$ accumulating in the chamber headspace from N_2O production can cause a smaller observed loss of the $^{15}N_2O$ tracer at high N_2O production rates, leading to underestimates of N_2O consumption rates. Second, discrimination against reduction of $^{15}N_2O$ can cause a lower observed dilution of the $^{15}N_2O$ pool at

high N_2O consumption rates, leading to underestimates of gross N_2O production. Theoretically, these problems can be avoided by increasing the ^{15}N enrichment of the chamber headspace N_2O pool to a level at which the accumulation of $^{15}N_2O$ becomes trivial against the initial $^{15}N_2O$ pool and atom% ^{15}N enrichment. However, to further enrich the $^{15}N_2O$ pool, we would also further increase the chamber headspace N_2O concentration and risk stimulating N_2O consumption. Thus, we addressed these potential problems by using k_{15} as a floating variable rather than a fixed variable in the model so that k_{15} was estimated by the model using the observed k_{15} as an initial value (i.e. the second approach described above).

Site description

We tested the $^{15}N_2O$ pool dilution technique in a managed grassland that had previously exhibited high N_2O emissions (average 6.4 ± 0.4 mg N m^{-2} day^{-1}; Teh *et al*., 2011). This suggested that site had the potential for high total denitrification rates and would exhibit N_2O dynamics ideal for testing the technique. The study site is located on Sherman Island (38.04 N, 121.75 W) in the Sacramento–San Joaquin River Delta region of northern California. The climate is Mediterranean with a winter wet season. The mean annual temperature is 15.6 °C, and the mean annual precipitation is 325 mm (Teh *et al*., 2011). The soils consist of an oxidized layer over buried peat and are classified as fine, mixed, superactive, thermic Cumulic Endoaquolls (Drexler *et al*., 2009). We divided the study area (0.38 km^2) into four microtopographical landforms that differ primarily in drainage characteristics: crown, slope, hollow/hummock, and irrigation ditch (from faster to slower drainage).

Diffusion modeling

We modeled vertical diffusive transport of the $^{15}N_2O$ tracer through the soil profile using the analytical solution for the Fick's law equation presented by von Fischer *et al.* (2009). Soil tortuosity was calculated for each landform on each sampling date using the Millington & Quirk (1961) model, which uses soil bulk density and moisture as parameters. We used soil bulk density values previously measured across all four landforms (Y. Teh, unpublished data) and gravimetric soil moisture measured from each flux chamber measurement. Nitrous oxide diffusivity in air at standard temperature and pressure is 0.1436 cm^2 s^{-1} and changes with temperature according to the scaling factor, $(T/T_0)^{1.81}$ (Massman, 1998). The free-air N_2O diffusion coefficient at 15 °C, 0.1582 cm^2 s^{-1}, was used. We modeled diffusion over a 22.5 min time period because we are interested in the potential for the tracer to diffuse through the soil and then back into the chamber headspace during a 45 min sampling period. This accounts for the tracer diffusing to a certain depth in the first 22.5 min and then diffusing back to the soil surface in the next 22.5 min. This model does not account for lateral movement of the tracer which becomes important at longer time scales (von Fischer *et al*., 2009).

Laboratory methods

We measured ammonium (NH_4^+) and NO_3^- concentrations as well as denitrification enzyme activity (DEA) in depth profiles in the crown and slope landforms to determine spatial patterns in substrate availability and potential denitrifier activity. We sampled two profiles within each of five replicate plots (1 m diameter) located 10 m apart on a transect in each landform. For each profile, we bulked soil from 20 cm depth intervals down to the water table at 60 cm depth. The soils were transported to UC-Berkeley (UCB) in gas permeable bags at ambient temperature and assayed the next day as detailed below.

In the laboratory, each soil core was homogenized, and ca. 15 g soil (oven dry equivalent) was extracted in 75 mL of 2 M KCl. The 2 M KCl extracts were analyzed colorimetrically for NO_3^- and NH_4^+ (Lachat Quik Chem flow injection analyzer; Lachat Instruments, Milwaukee, WI, USA). A 10 g subsample from each core was oven-dried at 105 °C for determination of gravimetric soil water content. DEA was measured according to a modified protocol based on those described in Tiedje (1994) and Silver *et al*. (2000): 100 mL of de-gassed 1 mM glucose, 1 mM KNO_3, and 1 g L^{-1} chloramphenicol in DI water to 20 g soil in a 250 mL Mason jar. The jar was sealed with a lid equipped with a rubber septum port, and then it was flushed with N_2 for 3 min to create an anaerobic headspace. Acetylene (C_2H_2) was added to achieve a concentration of 10 kPa. The jar was shaken to slurry the soil and then placed on an orbital shaker at 100 rpm. The jar headspace was sampled at 10, 20, 30, and 40 min after vigorously shaking the jar each time and the gas samples were analyzed for N_2O concentration. Denitrifying enzyme activity was calculated from the linear increase in N_2O concentration over time.

In the laboratory, we compared the $^{15}N_2O$ pool dilution technique against two existing methods for measuring N_2 production, C_2H_2 inhibition and $^{15}NO_3^-$ tracer. While both of these methods have well-recognized shortcomings (Groffman *et al*., 2006), they can provide general benchmarks for comparison. For the C_2H_2 inhibition technique, we used three headspace treatments: 0 Pa C_2H_2 (control), 10 Pa C_2H_2 (nitrification inhibited), and 10 kPa C_2H_2 (nitrification + N_2O reduction inhibited). The C_2H_2 was produced by adding deionized water to calcium carbide in an evacuated gas bag. For the $^{15}NO_3^-$ tracer technique, 2 mL of 99.7 atom% ^{15}N–potassium nitrate (KNO_3) solution was added to soil, which increased the NO_3^- concentration by 5 μg N g^{-1}. The soil was lightly mixed to distribute the ^{15}N label. For the $^{15}N_2O$ pool dilution technique, 5 mL of a 98 atom% $^{15}N_2O$ spiking gas was added to increase the headspace N_2O concentration by 1 ppm.

Soil was collected from 0 to 10 cm depth in the crown topographic zone and stored in a gas permeable bag at ambient conditions for 5 days before the experiment. The soil was gently homogenized, preserving aggregates up to 1 cm diameter and then 100 g was weighed into each sample jar (490 mL). The jars were sealed on viton gaskets with aluminum lids equipped with Swagelok o-seal fittings containing septa for gas sampling. The jars were flushed with N_2 to create an anaerobic headspace and then the appropriate gas treatment was added.

For the C_2H_2 inhibition and $^{15}N_2O$ pool dilution treatments, the jars were sampled at 0.25, 1, 2, and 3 h. For $^{15}NO_3^-$ tracer

treatment, the jars were only sampled at 0.25 and 3 h because detectable changes in $^{15}N–N_2$ atom% were not expected at earlier time points based on net N_2O fluxes previously measured at the study site (Teh *et al*., 2011). For all treatments, 60 mL headspace gas was removed and stored in a pre-evacuated glass Wheaton vial sealed with an aluminum crimp and a Teflon coated septum; 60 mL ultra-high purity helium (He) was injected into the incubation jars to keep the headspace at atmospheric pressure without changing the isotopic composition of the headspace N_2 or N_2O. For the C_2H_2 treatments, C_2H_2 was also added back to maintain the desired C_2H_2 concentration. We corrected for the dilution of headspace gases caused by adding He.

Field methods

We performed eight pairs of field measurements in the crown and slope zones in February 2009 to determine if N_2O dynamics were affected by increasing the N_2O concentration in the surface flux chamber headspace for the $^{15}N_2O$ pool dilution technique. For each pair, we measured net N_2O fluxes with and without the injection of spiking gas ($^{15}N_2O$ and SF_6 in N_2), allowing the soil to re-equilibrate with the atmosphere for 1 h between the two measurements. We reversed the order of the measurements for half of the pairs to avoid systematic bias in the measurements. We compared net N_2O fluxes with and without the spiking gas injection using regression analysis; a slope for the regression line deviating from unity would suggest a significant effect of spiking gas injection on N_2O dynamics. We also evaluated the accuracy of the $^{15}N_2O$ pool dilution technique using regression analysis to compare the measured and estimated net N_2O fluxes for the spiked measurements (including measurements from later sampling dates). Estimated net N_2O flux was determined as the difference between gross N_2O production and consumption rates estimated by the $^{15}N_2O$ pool dilution technique described below. This comparison allowed us to evaluate how well the estimated net N_2O fluxes fit measured net N_2O fluxes. If the estimated net N_2O fluxes were significantly higher than measured net N_2O fluxes, then this would suggest that gross N_2O production rates were overestimated and/or gross N_2O consumption rates were underestimated by the $^{15}N_2O$ pool dilution model. If the estimated net N_2O fluxes were significantly lower than measured net N_2O fluxes, then this would suggest that gross N_2O production rates were underestimated and/or gross N_2O consumption rates were overestimated.

Twelve $^{15}N_2O$ pool dilution measurements were performed across all landforms (n = 3 per landform) in March 2009 and again in April 2009. For field measurements, we used a two-piece aluminum static flux chamber with a square basal area of 0.14 m^2 and approximate volume of 17 L. The chamber lid was equipped with two fans, a 60 cm long 1/8″ stainless steel pigtail vent that could be sealed, and two septum ports (one for sampling and one for spiking gas injection). The chamber was covered in two layers of reflective bubble wrap to minimize heating of the chamber headspace under sunny conditions. The chamber sealed on a 1/8″ thick viton gasket using spring clamps or C-clamps. The leak rate from the chamber was determined to be 0.3% per hour by placing the sealed chamber over a tray of water, injecting SF_6, and determining the change in SF_6 concentration over 3 h.

The chamber base was inserted ca. 3 cm into the soil and allowed to equilibrate for 30–45 min before sampling. The chamber lid was then sealed to the base and the fans turned on to mix the chamber headspace. We injected 10 mL of spiking gas at 100 ppm of 98 atom% $^{15}N–N_2O$ and 10 ppm of SF_6 through a septum port in the chamber lid using a syringe. This increased chamber headspace concentrations by ca. 60 ppb N_2O and 6 ppb SF_6 and increased the ^{15}N-enrichment of the headspace N_2O by ca. 14 atom%. The spiking gases were made volumetrically in gas bags using certified 99.8% of 98 atom% $^{15}N–N_2O$ (Isotech), 99.8% SF_6 (Scotty Specialty Gases), and ultra-high purity N_2 (Praxair).

The chamber headspace was sampled from a different septum port in the chamber lid at 3, 8, 15, 30, and 45 min after spiking gas injection. The vent was sealed when the chamber was not being sampled so that loss of $^{15}N_2O$ and SF_6 through the vent could be minimized. The samples were stored in pre-evacuated glass vials sealed with aluminum crimps and Teflon septa. The vial septa were immediately coated in silicone sealant to minimize the potential for leakage and the samples were stored for up to 5 days before analysis.

After the last sampling time point, we measured the temperature of the ambient air, chamber headspace, and soil (0–10 cm depth). The chamber height was measured at three points along each side of the chamber and then averaged to calculate the chamber volume. Four 5 cm diameter soils cores (0–10 cm depth) were taken, one from each quadrant of the chamber footprint. The intact cores were transported to UCB in gas permeable bags at ambient temperature and processed on the same day for NH_4^+ and NO_3^- concentrations, soil moisture, and DEA as previously described. In addition, pH of air-dried soil was measured using 10 g soil in a 4 : 1 ratio of 1 M KCl to air-dried soil.

In April 2009, we measured soil oxygen (O_2) concentrations from twelve soil O_2 chambers based on the design described by Silver *et al*. (1999). The chambers consisted of a polypropylene centrifuge tube (3 cm diameter and 12 cm length) with a 1/8″ Swagelok union inserted through a hole drilled into the round end. The union was sealed to the tube with marine goop, and a septum was inserted into the fitting on the exposed side of the union. The chambers were pushed into 10 cm deep holes slightly wider in diameter than the chamber so that the bottom 2 cm of the chamber was filled with soil and the Swagelok end barely protruded from the soil surface. Soil was packed back in around the chambers to create a seal against atmospheric air. The chambers were allowed to equilibrate for 1 week before sampling. A 30 mL gas sample was drawn from the chamber and immediately analyzed using a dissolved O_2 meter (Model 52; Yellow Springs Instruments, Yellow Springs, OH, USA) and Clark-type electrode fitted with an airtight cell. The electrode was calibrated in the field using atmospheric air as well as ultra-high purity N_2 stored in a gas bag. Each of the surface flux measurements in April 2009 were taken within 50 cm of a soil O_2 chamber.

Gas analyses

In February 2009, when we performed method testing in the field, samples were analyzed for N_2O isotopic composition on a PDZ Europa 20-20 IRMS (Crewe, UK) and a SerCon Cryoprep trace gas concentration system (Crewe, UK) at the University of California, Davis Stable Isotope Facility. For the rest of the samples, isotope analyses were performed at UCB on an PDZ Europa IRMS with a manually operated custom-built trace gas concentration system that included a liquid nitrogen trap and a 25 m × 0.32 mm Poraplot Q column operated at 30 °C. $^{15}N_2$ analyses were performed on the UCB IRMS by directly injecting 100 μL sample into the He carrier stream upstream of a heated copper reduction tube to remove O_2; samples were injected using a glass gas-tight syringe with a zero-volume stopcock. Samples were analyzed for N_2O, SF_6, and carbon dioxide (CO_2) concentrations on a Shimadzu GC-14A equipped with an electron capture detector (ECD) and thermal conductivity detector at UCB. A 4 m × 1 mm Hayesep Q column was used to allow adequate peak separation between N_2O and SF_6 on the ECD. We used a 10.1 ppb SF_6 in N_2 standard gas as well as a 998 ppm CO_2, 10.4 ppm N_2O in N_2 standard gas for one-point calibrations because previous work showed that the detector responses were linear in the concentration range of our samples and standards.

Statistical analysis

We used SYSTAT Version 10 (SPSS Inc., Evanston, IL, USA) to perform statistical analyses and the Microsoft Excel 2007 (Microsoft Corporation, Redmond, WA, USA) to run the iterative pool dilution model. We log-transformed variables with non-normal distributions (all except soil moisture, soil O_2, and pH) to meet the normality assumptions of ANOVA and linear regressions. We used ANOVA and Tukey tests to compare N_2O dynamics and soil variables among the four landforms as well as to compare soil characteristics among the depth intervals measured in the soil profiles. We used linear regressions to explore patterns in N_2O and N_2 dynamics with possible explanatory variables including soil O_2, NO_3^-, and NH_4^+ concentrations; CO_2 emissions (as a proxy for labile C availability); pH; soil moisture; soil and air temperature; and gross N_2O production rates. Mean values are reported in the text followed by standard errors (±SE). Statistical significance was determined at $P < 0.05$ unless otherwise noted.

Results

Method evaluation

In the laboratory, gross N_2O production and consumption rates estimated by $^{15}N_2O$ pool dilution were 2.29 ± 0.68 and 0.12 ± 0.09 μg g^{-1} day^{-1}, respectively. By contrast, gross N_2O consumption rates calculated from the difference between estimated gross N_2O production rates and measured net N_2O fluxes (1.13 ± 0.50 μg g^{-1} day^{-1}) averaged 1.17 ± 0.84 μg g^{-1} day^{-1}. The estimated gross N_2O production rates and calculated gross N_2O consumption rates from $^{15}N_2O$ pool dilution were not significantly different than gross N_2O production and consumption rates estimated using the C_2H_2 inhibition technique (3.91 ± 1.30 and 3.27 ± 1.32 μg g^{-1} day^{-1}, respectively). Gross N_2O production and consumption rates estimated by the $^{15}NO_3^-$ tracer method (10.62 ± 1.41 and 10.58 ± 1.41 μg g^{-1} day^{-1}, respectively) were significantly higher than those estimated by $^{15}N_2O$ pool dilution and C_2H_2 inhibition ($P < 0.05$). The background soil NO_3^- concentration was 2.0 ± 1.0 μg N g^{-1} so the addition of 5 μg ^{15}N–NO_3^- g^{-1} for the $^{15}NO_3^-$ tracer method increased the soil NO_3^- by a factor of 2.5. Measured net N_2O fluxes (0.46 ± 0.27 μg g^{-1} day^{-1} for C_2H_2 inhibition and 0.77 ± 0.97 μg g^{-1} day^{-1} for $^{15}NO_3^-$ tracer) did not differ significantly among the three methods tested.

In the field, increasing the N_2O concentration of the chamber headspace by up to 100 ppb did not significantly alter net N_2O fluxes. Across the eight pairs of measurements unspiked and spiked with $^{15}N_2O$, net N_2O fluxes decreased by 1 ± 2% (Fig. 1a). Observed $^{14}N_2O$ concentrations across all sampling time points were strongly correlated with $^{14}N_2O$ concentrations predicted by the pool dilution model to estimate gross N_2O production rates ($R^2 = 1$, $y = 1.003x + 0.008$). Observed $^{15}N_2O$ concentrations were also strongly correlated with $^{15}N_2O$ concentrations predicted by the pool dilution model ($R^2 = 0.91$, $y = 1.044x + 0.003$). SF_6 and $^{15}N_2O$ concentrations Estimated net N_2O fluxes, 4 calculated as the difference between gross N_2O production and consumption rates estimated by the pool dilution model, were 11 ± 1% greater than measured net N_2O fluxes (Fig. 1b).

Using a diffusion model, we estimated that the $^{15}N_2O$ and SF_6 concentrations in the soil reached at least 10% of the initial headspace concentrations to 63 cm soil depth within 22.5 min in soils with the highest diffusivity. In soils with the lowest diffusivity, tracer concentrations were at least 10% of the initial headspace concentrations only to 15 cm depth. The tracer concentrations reached at least 1% of the initial headspace concentrations at maximum depths of 23 cm to >70 cm. The range in tracer penetration into the soil profile was due to differences in soil bulk density and soil moisture that affected soil diffusivity, which ranged from 2.5 to 6.6 cm^2 min^{-1}.

Gross nitrous oxide fluxes: field rates and controls

We observed high N_2O emissions across all landforms and sampling dates, averaging 6.4 ± 2.6 mg N m^{-2} day^{-1}. Gross N_2O production rates averaged 8.4 ±

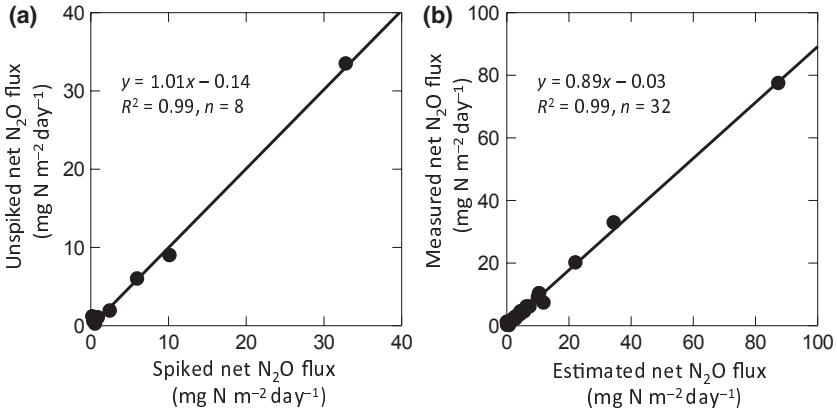

Fig. 1 (a) Net N_2O flux without $^{15}N_2O$ spiking gas addition vs. net N_2O flux with $^{15}N_2O$ spiking gas addition. (b) Measured net N_2O flux (from change in chamber headspace N_2O concentration over time) vs. estimated net N_2O flux (from difference between predicted gross N_2O production and consumption rates). Regression lines are shown in each panel.

3.2 mg N m^{-2} day^{-1} across landforms and sampling dates. Nitrous oxide emissions were significantly lower in the slope compared with the crown and irrigation ditch ($P < 0.001$). Gross N_2O production rates were greatest in the crown zone compared with all of the other landforms ($P = 0.1$; Fig. 2).

Gross N_2O consumption was a relatively small proportion of gross N_2O production (Fig. 2). As expected, gross N_2O consumption rates were underestimated using the pool dilution approach when compared with rates calculated as the difference between gross and net N_2O production rates. Calculated N_2O consumption rates averaged 2.0 ± 0.8 mg N m^{-2} day^{-1} and rates estimated by the pool dilution model were 55 ± 1% lower. The N_2O yield (i.e. the proportion of gross N_2O production released to the atmosphere) averaged 0.70 ± 0.04 using calculated N_2O consumption rates and 0.84 ± 0.03 using the estimated gross consumption rates. Calculated gross N_2O consumption rates were greater in the crown compared with the hollow/hummock ($P = 0.04$) but did not differ significantly among the other landforms. The N_2O yield did not differ significantly among landforms.

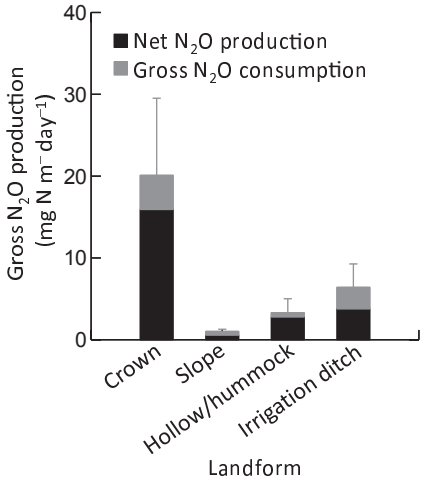

Fig. 2 Mean gross N_2O production rates across all sampling dates and by landform are shown by the cumulative bars. The landforms are presented in order of decreasing drainage. The gray portion of the bars represents calculated gross N_2O consumption rates and the black portion of the bars represents measured net N_2O production rates. Error bars represent standard errors for gross N_2O production rates.

Most soil characteristics varied significantly among landforms (Table 1). Gravimetric soil moisture content was lower in the crown and slope compared with the hollow/hummock and irrigation ditch, with landform means ranging from 0.29 to 0.48 g H_2O g^{-1} ($P < 0.001$). Soil mineral N concentrations averaged 27 ± 8 μg N g^{-1} overall. Soil NH_4^+ concentrations were highly variable (Table 1) and thus did not differ significantly among landforms; soil NO_3^- concentrations were higher in the crown compared with the other landforms ($P < 0.001$). Soil pH also varied among landforms (Table 1), with higher pH in the crown than in the slope ($P = 0.03$). Soil O_2 concentrations were spatially heterogeneous within and across landforms (1–20%), except for the slope where soil O_2 concentrations were all relatively aerobic, averaging 17 ± 1%. Denitrifying enzyme activity was lower in the slope compared with the irrigation ditch ($P = 0.04$) and was most strongly correlated to pH ($R^2 = 0.72$; Fig. 3). The combination pH and soil O_2 concentration explained 91% of the variability in DEA (Table 2).

We sampled soil depth profiles in the crown (highest N_2O fluxes) and slope (lowest N_2O fluxes) to explore patterns in DEA and substrate availability with depth. Denitrifying enzyme activity was greater in surface

Table 1 Soil characteristics (0–10 cm depth) by landform

Landform	*n*	Soil moisture (g H_2O g^{-1})	Soil pH	Soil NO_3^- concentration (μg N g^{-1})	Soil NH_4^+ concentration (μg N g^{-1})	N_2O yield	Denitrifying enzyme activity (μg N g^{-1} h^{-1})
Crown	10	0.29 ± 0.02 a	5.46 ± 0.12 a	14.65 ± 4.36 a	44.73 ± 20.05 a	0.68 ± 0.08	1.23 ± 0.53 ab
Slope	10	0.35 ± 0.02 a	5.08 ± 0.05 b	1.25 ± 0.34 b	5.92 ± 1.50 a	0.60 ± 0.08	0.19 ± 0.02 b
Hollow/ hummock	6	0.46 ± 0.04 b	5.19 ± 0.12 ab	0.69 ± 0.18 b	9.56 ± 5.46 a	0.87 ± 0.06	0.53 ± 0.13 ab
Irrigation ditch	6	0.48 ± 0.02 b	5.36 ± 0.05 ab	0.88 ± 0.39 b	19.19 ± 7.03 a	0.71 ± 0.10	0.71 ± 0.11 a

Means ± standard errors are reported. Letters indicate significant differences at $P < 0.05$.

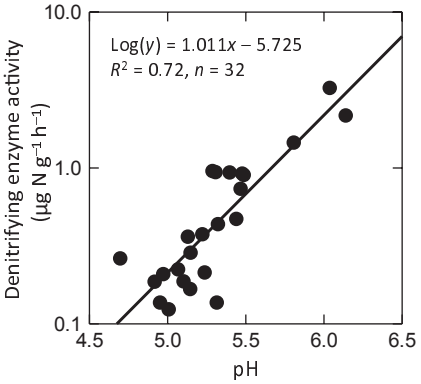

Fig. 3 Log-transformed denitrifying enzyme activity vs. pH. The linear regression line is shown.

soils (0–20 cm depth) compared with soils at depth (20–40 and 40–60 cm; $P = 0.003$, $n = 10$; Fig. 4a). Mineral N concentrations tended to be lower with soil depth but did not differ significantly among soil depths (Fig. 4b).

Across landforms, mineral N concentration was the strongest predictor of gross N_2O production ($R^2 = 0.57$; Fig. 5a). Mineral N concentration together with DEA explained 73% of the variability in gross N_2O production (Table 2). As a single variable, DEA had a strong positive relationship with gross N_2O production ($R^2 = 0.47$; Fig. 5b), but only a weak positive relationship with calculated gross N_2O consumption ($R^2 = 0.25$). Calculated gross N_2O consumption rates were most strongly correlated to gross N_2O production ($R^2 = 0.61$; Table 2). There were no statistically significant relationships between the measured soil characteristics and N_2O yields.

Discussion

Method evaluation

Gross N_2O production and consumption rates measured in the laboratory were comparable using the $^{15}N_2O$ pool dilution and acetylene inhibition methods. Not surprisingly, the large $^{15}NO_3$ addition necessary to detect changes in $^{15}N_2$ caused greater measured gross N_2O production and consumption rates when using the $^{15}NO_3^-$ tracer method compared with the other methods. Acetylene inhibition can sometimes underestimate N_2O consumption to N_2 for a variety of reasons, including limited diffusion of C_2H_2 to microsites of denitrification, the ineffectiveness of C_2H_2 in blocking N_2O reduction in some organisms and the metabolism of C_2H_2 (Knowles, 1990). Thus, the fact that N_2O consumption rates measured by $^{15}N_2O$ pool dilution were not lower than those measured by acetylene inhibition (which tends to underestimate consumption) or higher than those measured by $^{15}NO_3^-$ tracer (which tends to overestimate consumption) suggests that $^{15}N_2O$ pool

Table 2 Linear regressions describing predictors of N_2O dynamics

Dependent variable	Independent variable	Regression coefficient (±SE)	*P*-value	*n*	R^2
Log(gross N_2O production, μg N m^{-2} day^{-1})	Constant	2.88 ± 0.24	<0.01	24	0.73
	Log(mineral N concentration, μg N g^{-1})	0.73 ± 0.16	<0.01		
	Log(DEA, μg N g^{-1} h^{-1})	0.57 ± 0.22	<0.01		
Log(1 + N_2O consumption, μg N m^{-2} day^{-1})	Constant	0.01 ± 0.07	0.83	32	0.61
	Log(gross N_2O production)	0.59 ± 0.09	<0.01		
Log(DEA)	Constant	−3.39 ± 0.79	<0.01	12	0.91
	pH	0.65 ± 0.14	<0.01		
	Log(soil O_2 concentration)	−0.03 ± 0.01	<0.01		

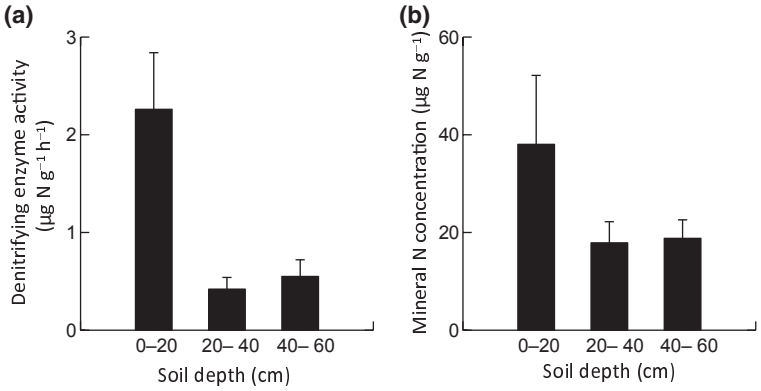

Fig. 4 (a) Mean denitrifying enzyme activity and (b) mean mineral N concentration for 20 cm soil depth intervals (n = 10). Error bars represent standard errors and letters represent significant differences among soil depths.

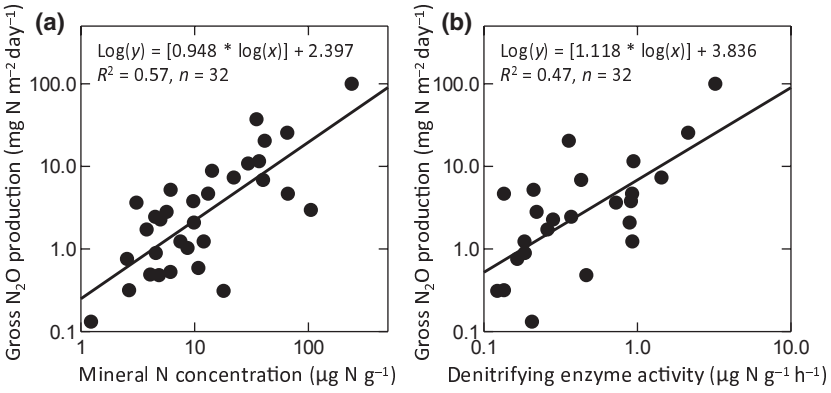

Fig. 5 Log-transformed gross N_2O production rates vs. (a) log-transformed mineral N concentration and vs. (b) log-transformed denitrifying enzyme activity. Regression lines are shown in each panel.

dilution technique provides reasonable estimates of N_2O dynamics.

The addition of $^{15}N_2O$ to the chamber headspace N_2O concentration (up to 100 ppb) did not significantly impact measured net N_2O fluxes. Due to the high N_2O production rates at our study site, we added a relatively large amount of $^{15}N_2O$ to the chamber headspace to minimize the potential for the $^{15}N_2O$ pool to be isotopically diluted down to natural abundance ^{15}N enrichment levels before the end of the sampling period. Isotopic dilution to near natural abundance ^{15}N enrichment would have caused difficulties in accurately modeling the change in the ^{15}N isotopic composition of the chamber headspace N_2O over time (von Fischer & Hedin, 2002).

One test of the $^{15}N_2O$ pool dilution model is a comparison of measured net N_2O fluxes with net N_2O fluxes calculated as the difference between gross N_2O production and consumption rates estimated by the pool dilution model. Net N_2O fluxes estimated by the pool dilution technique were on average 11% greater than the observed net N_2O fluxes, which is a relatively small error compared with the variability in net N_2O fluxes that spanned four orders of magnitude at this site. The greater estimated net N_2O fluxes reflect overestimates of gross N_2O production and/or underestimates of N_2O consumption. Gross N_2O production rates are unlikely to be overestimated using the pool dilution technique because anomalously fast isotopic dilution of the $^{15}N_2O$ pool is improbable. A comparison of estimated and calculated gross N_2O consumption rates suggests that the $^{15}N_2O$ pool dilution technique underestimated N_2O consumption rates by ca. 55%. Underestimates of N_2O consumption using the $^{15}N_2O$ pool dilution technique could occur as a result of limited $^{15}N_2O$ diffusion to microsites of denitrification or complete denitrification of NO_3^- to N_2 intracellularly. We therefore deduce that calculated N_2O consumption rates more accurately reflect actual gross N_2O consumption rates.

We used multiple approaches to explore factors that contribute to errors in the gross N_2O consumption rates estimated by the pool dilution model. We found that DEA was significantly greater in the top 20 cm of soil in both the crown and slope zones, which spanned the highest and lowest gross N_2O production rates. Mineral N concentrations exhibited a similar though not statistically significant trend. These data suggest that gross N_2O production and consumption rates were likely greatest in surface soils, which is consistent with depth profile measurements of N_2O and N_2 production as well as denitrification potential in similar managed grasslands (Koops *et al*., 1996, 1997; van Beek *et al*., 2004). Vertical diffusion modeling suggested that we achieved a tracer concentration of ca. 10% of the initial chamber headspace concentration at 15–63 cm depth in the soil within half of the flux measurement time (22.5 min), depending on the estimated soil diffusivity. The water table fluctuates between 30 to 70 cm depth at our study site (Deverel *et al*., 2007). This suggests that in many cases the tracer was able to penetrate the unsaturated soil profile. Thus, heterogeneous tracer distribution that followed the same trend as N_2O dynamics within the soil profile likely led to a moderate error in gross N_2O consumption rates estimated by the pool dilution technique (Davidson *et al*., 1991). Inadequate tracer movement to soil depth may have contributed to underestimates in the gross N_2O consumption rates measured in sampling locations with wetter and more compacted soil. To address this issue, a longer sampling time period could be used to allow the $^{15}N_2O$ tracer to diffuse deeper into the soil profile. This should be accompanied by a deeper insertion of the chamber into the soil to reduce lateral diffusion of the tracer, which increases with time (von Fischer *et al*., 2009).

Although the $^{15}N_2O$ pool dilution model solves for gross N_2O production and consumption rates simultaneously, the error in N_2O consumption rates would not cause substantial error in estimated gross N_2O production rates for several reasons. First, inadequate or heterogeneous $^{15}N_2O$ tracer diffusion into soil microsites of denitrification does not affect rates of isotopic dilution of the chamber headspace $^{15}N_2O$ pool, which is used to estimate gross N_2O production rates. Second, the consumption of N_2O weakly discriminates against $^{15}N_2O$ ($\alpha = 0.9924 \pm 0.0036$; see Table S3) so that the accumulation of $^{15}N_2O$ in the chamber headspace due to discrimination against ^{15}N during N_2O consumption should have a small impact on the ^{15}N enrichment of the N_2O pool. Third, the pool dilution model estimated $^{14}N_2O$ concentrations that fit the observed $^{14}N_2O$ concentrations very well; estimated $^{15}N_2O$ concentrations also fit observed $^{15}N_2O$ concentrations well. This suggests that the model provided robust estimates of gross N_2O production rates.

The average N_2O yield estimated from calculated N_2O consumption rates was 0.70 ± 0.04, suggesting that a large proportion of soil N_2O is released to the atmosphere rather than being denitrified to N_2 at our study site. High soil NO_3^- concentrations can inhibit N_2O consumption, resulting in high N_2O yields (Blackmer & Bremner, 1978; Firestone *et al*., 1979, 1980; Weier *et al*., 1993). The high soil mineral N concentrations at our study site were dominated by NH_4^+ rather than NO_3^-, but high gross nitrification rates at the site (E. Portier and W. Yang, unpublished data) could supply ample NO_3^- for incomplete denitrification.

N_2O dynamics

We observed consistently high N_2O emissions that were comparable with those measured previously at this site (Teh *et al*., 2011) and reported for other relatively N-rich grasslands (e.g. Koops *et al*., 1997; van Beek *et al*., 2010). The magnitude of N_2O emissions results from both gross N_2O production rates and the relative importance of N_2O to N_2 as denitrification end-products (Firestone & Davidson, 1989). At this site, the high N_2O emissions reflected both high gross N_2O production rates and high N_2O yields.

Mineral N concentrations were very high in surface soils (0–10 cm depth) at this site and were the strongest predictor of gross N_2O production rates. Across all landforms, mineral N concentration together with DEA explained 73% of the variability in gross N_2O production rates. The strength of the relationship suggests that the N_2O was produced in surface soils rather than diffusing upward from groundwater below the vadose zone. Gross N_2O consumption rates were most strongly correlated to gross N_2O production rates and were not correlated with any of the properties measured in the bulk soil. It is possible that N_2O consumption may have occurred in soil microsites where localized NO_3^- limitation led to N_2O reduction. Nitrous oxide yields were also not related to any soil properties we measured. In laboratory studies, the ratio of N_2O : N_2 emissions has been related to O_2 concentrations, redox, pH, NO_3^- availability, and labile C availability (Firestone *et al*., 1979, 1980; Weier *et al*., 1993; Del Grosso *et al*., 2000). However, in the field where heterogeneous soil conditions occur, the controls on N_2O consumption, and thus the N_2O yields, may be more complex.

The crown landform exhibited the highest N_2O emissions and the highest mineral N concentrations. This is the only landform on which the invasive pepperweed, *Lepidium latifolium*, was found at the time of the study. Pepperweed can stimulate microbial enzyme activity to

increase soil N mineralization and thus mineral N concentrations (Blank, 2002; Blank & Young, 2004). Nitrous oxide emissions in these soils could increase in the future, if the pepperweed invasion spreads downslope (Sonnentag *et al*., 2011).

Conclusions

The $^{15}N_2O$ pool dilution technique has never before been applied in upland soils or in the field setting. Here we demonstrated that the $^{15}N_2O$ pool dilution technique provides robust field and laboratory estimates of gross N_2O production rates across a wide range of gross N_2O fluxes and soil characteristics. A major advantage of this technique is that it allows for the measurements of N_2O dynamics in unmanipulated soil so that rates of nitrification and denitrification are not altered by changes in redox conditions. Gross N_2O consumption rates were significantly underestimated by the pool dilution model, likely due in part to heterogeneous ^{15}N tracer distribution within the soil profile and inadequate ^{15}N tracer diffusion to sites of N_2O consumption. However, we obtained reasonable estimates of N_2O consumption rates calculated from the difference between gross N_2O production and net N_2O fluxes. These two approaches to estimating gross N_2O consumption rates provided well-constrained estimates of the N_2O yield for this site.

The high N_2O emissions observed in the managed grassland studied here are likely a result of high mineral N concentrations that drove high rates of incomplete denitrification in the surface soils. The drivers of the N_2O yield, however, were less clear. It is critical to understand the controls on N_2O dynamics in ecosystems with high N_2O emissions because these ecosystems have substantial impacts on atmospheric N_2O concentrations. However, this method could also be applied to ecosystems with low N_2O emissions and potentially provide insight into the growing evidence of net N_2O uptake by soils (Chapuis-Lardy *et al*., 2007). The $^{15}N_2O$ pool dilution approach provides a valuable tool for estimating gross N_2O fluxes and N_2O yield under field conditions and will likely facilitate future experiments to identify drivers of these important N dynamics.

Acknowledgements

We appreciate advice and suggestions from M. K. Firestone and R. C. Rhew that improved this study and manuscript. We received assistance in the field and laboratory from M. Almaraz, S. Hall, A. McDowell, E. Portier, and B. Quintero. This research was funded by grants ATM-0842385 and DEB-0543558 to W. L. S. and DDIG 0808383 to W. H. Y. from the U.S. National Science Foundation (NSF). W. H. Y. was supported by an NSF Graduate Research Fellowship.

References

Addy K, Kellogg DQ, Gold AJ, Groffman PM, Ferendo G, Sawyer C (2002) In situ push-pull method to determine ground water denitrification in riparian zones. *Journal of Environmental Quality*, **31**, 1017–1024.

Addy K, Gold A, Nowicki B, McKenna J, Stolt M, Groffman P (2005) Denitrification capacity in a subterranean estuary below a Rhode Island fringing salt marsh. *Global Change Biology*, **28**, 896–908.

van Beek CL, Hummelink EWJ, Veltoh GL, Oenema O (2004) Denitrification rates in relation to groundwater level in a peat soil under grassland. *Biology and Fertility of Soils*, **39**, 329–336.

van Beek CL, Pleijter M, Jacobs CMJ, Velthof GL, von Groenigen JW, Kuikman PJ (2010) Emissions of N_2O from fertilized and grazed grassland on organic soil in relation to groundwater level. *Nutrient Cycling in Agroecosystems*, **86**, 331–340.

Blackmer AM, Bremner JM (1978) Inhibitory effect of nitrate on reduction of N_2O to N_2 by soil microorganisms. *Soil Biology and Biochemistry*, **10**, 187–191.

Blank RR (2002) Amidohydrolase activity, soil N status, and the invasive crucifer *Lepidium latifolium*. *Plant and Soil*, **239**, 155–163.

Blank RR, Young JA (2004) Influence of three weed species on soil nutrient dynamics. *Soil Science*, **169**, 385–397.

Bollmann A, Conrad R (1998) Influence of O_2 availability on NO and N_2O release by nitrification and denitrification in soils. *Global Change Biology*, **4**, 387–396.

Booth MS, Stark JM, Rastetter E (2005) Controls on nitrogen cycling in terrestrial ecosystems: a synthetic analysis of literature data. *Ecological Monographs*, **75**, 139–157.

Boyer EW, Alexander RB, Parton WJ *et al*. (2006) Modeling denitrification in terrestrial and aquatic ecosystems at regional scales. *Ecological Applications*, **16**, 2123–2142.

Chapuis-Lardy L, Wrage N, Metay A, Chotte JL, Bernoux M (2007) Soils, a sink for N_2O? A review. *Global Change Biology*, **13**, 1–17.

Clough TJ, Kelliher FM, Wang YP, Sherlock RR (2006) Diffusion of ^{15}N-labelled N_2O into soil columns: a promising method to examine the fate of N_2O in subsoils. *Soil Biology and Biochemistry*, **38**, 1462–1468.

Clough TJ, Addy K, Kellogg DQ, Nowicki BL, Gold AJ, Groffman PM (2007) Dynamics of nitrous oxide in groundwater at the aquatic-terrestrial interface. *Global Change Biology*, **13**, 1528–1537.

Davidson EA, Hart SC, Shanks CA, Firestone MK (1991) Measuring gross nitrogen mineralization, immobilization, and nitrification by ^{15}N isotope pool dilution in intact cores. *Journal of Soil Science*, **42**, 335–349.

Del Grosso SJ, Parton WJ, Mosier AR, Ojima DS, Kulmala AE, Phongpan S (2000) General model for N_2O and N_2 gas emissions from soils due to denitrification. *Global Biogeochemical Cycles*, **14**, 1045–1060.

Deverel SJ, Leighton DA, Finlay MR (2007) Processes affecting agricultural drainwater quality and organic carbon loads in California's Sacramento–San Joaquin Delta. *San Francisco Estuary and Watershed Science*, **5**, 1–25.

Drexler JZ, de Fontaine CS, Deverek SJ (2009) The legacy of wetland drainage on the remaining peat in the Sacramento-San Joaquin Delta, California, USA. *Wetlands*, **29**, 372–386.

Firestone MK, Davidson EA (1989) N_2O production and consumption in soil. In: *Exchange of Trace Gases between Terrestrial Ecosystems and the Atmosphere* (eds Andreae MO, Schimel DS), pp. 7–21. John Wiley and Sons, New York.

Firestone MK, Smith MS, Firestone RB, Tiedje JM (1979) The influence of nitrate, nitrite, and oxygen on the composition of the gaseous products of denitrification in soil. *Soil Science Society of America Journal*, **43**, 1140–1144.

Firestone MK, Firestone RB, Tiedje JM (1980) Nitrous oxide from soil denitrification: factors controlling its biological production. *Science*, **208**, 749–751.

von Fischer JC, Hedin LO (2002) Separating methane production and consumption with a field- based isotope pool dilution technique. *Global Biogeochemical Cycles*, **16**, 1034, doi: 10.1029/2001GB001448.

von Fischer JC, Butters G, Duchateau PC, Thelwell RJ, Siller R (2009) In situ measures of methanotroph activity in upland soils: a reaction-diffusion model and field observation of water stress. *Journal of Geophysical Research*, **114**, G01015, doi: 10.1029/2008JG000731.

Goreau TJ, Kaplan WA, Wofsy SC, McElroy MB, Valios FW, Watson SW (1980) Production of NO_2^- and N_2O by nitrifying bacteria at reduced concentrations of oxygen. *Applied and Environmental Microbiology*, **40**, 526–532.

Groffman PM, Altabet MA, Bohlke JK *et al*. (2006) Methods for measuring denitrification: diverse approaches to a difficult problem. *Ecological Applications*, **16**, 2091–2122.

Kaiser J, Rockmann T, Brenninkmeijer CAM (2003) Complete and accurate mass spectrometric isotope analysis of tropospheric nitrous oxide. *Journal of Geophysical Research*, **108**, 4476, doi: 10.1029/2003JD003613.

Kirkham D, Bartholomew WV (1954) Equations for following nutrient transformations in soil, utilizing tracer data. *Soil Science Society of America Proceedings*, **18**, 33–34.

Knowles R (1990) Acetylene inhibition technique: development, advantages, and potential problems. In: *Denitrification in Soil and Sediment* (eds Revsbech NP, Sorensen J), pp. 151–166. Plenum Press, New York.

Koops JG, Oenema O, van Beusichem ML (1996) Denitrification in the top and sub soil of grassland on peat soils. *Plant and Soil*, **184**, 1–10.

Koops JG, van Beusichem ML, Oenema O (1997) Nitrogen loss from grassland on peat soils through nitrous oxide production. *Plant and Soil*, **188**, 119–130.

Kulkarni MV, Groffman PM, Yavitt JB (2008) Solving the global nitrogen problem: it's a gas! *Frontiers in Ecology and the Environment*, **6**, 199–206.

Massman WJ (1998) A review of the molecular diffusivities of H_2O, CO_2, CH_4, CO, O_3, SO_2, NH_3, N_2O, NO, and NO_2 in air, O_2, and N_2 near STP. *Atmospheric Environment*, **32**, 1111–1127.

Millington RJ, Quirk JP (1961) Permeabiliy of porous solids. *Transactions of the Faraday Society*, **57**, 1200–1207.

Prather MJ, Derwent R, Ehhalt D, Fraser P, Sanhueza E, Zhou X (1995) Other trace gases and atmospheric chemistry. In: *Climate Change 1994* (eds Houghton JT *et al.*), pp. 73–126. Cambridge University Press, Cambridge.

Punshon S, Moore RM (2004) A stable isotope technique for measuring production and consumption rates of nitrous oxide in coastal waters. *Marine Chemistry*, **86**, 159–168.

Rhew RC, Abel T (2007) Measuring simultaneous production and consumption fluxes of methyl chloride and methyl bromide in annual temperate grasslands. *Environmental Science and Technology*, **41**, 7837–7843.

Rhew RC, Aydin M, Saltzman ES (2003) Measuring terrestrial fluxes of methyl chloride and methyl bromide using a stable isotope tracer technique. *Geophysical Research Letters*, **30**, 2103, doi: 10.1029/2003GL018160.

Schlesinger WH (2009) On the fate of anthropogenic nitrogen. *Proceedings of the National Academy of Sciences of the United Staes of America*, **106**, 203–208.

Silver WL, Lugo AE, Keller M (1999) Soil oxygen availability and biogeochemical cycling along elevation and topographical gradients in Puerto Rico. *Biogeochemistry*, **44**, 301–328.

Silver WL, Neff J, Veldkamp E, McGroddy M, Keller M, Cosme R (2000) The effects of soil texture on below ground carbon and nutrient storage in a lowland Amazonian forest ecosystem. *Ecosystems*, **3**, 193–209.

Smith MS, Tiedje JM (1979) Phases of denitrification following oxygen depletion in soil. *Soil Biology & Biochemistry*, **11**, 261–267.

Sonnentag O, Detto M, Runkle BRK, Teh YA, Silver WL, Kelly M, Baldocchi DD (2011) Carbon dioxide exchange of a pepperweed (*Lepidium latifolium* L.) infestation: how do flowering and mowing affect canopy photosynthesis and autotrophic respiration? *Journal of Geophysical Research-Biogeosciences*, **116**, G01021, doi: 10.1029/2010JG001522.

Stein LY, Yung YL (2003) Production, isotopic composition, and atmospheric fate of biologically produced nitrous oxide. *Annual Review in Earth and Planetary Sciences*, **31**, 329–356.

Teh YA, Silver WL, Sonnentag O, Detto M, Kelly M, Baldocchi DD (2011) Large greenhouse gas emissions from a temperate peatland pasture. *Ecosystems*, **14**, 311–325.

Tiedje JM (1994) Denitrifiers. In: *Methods of Soil Analysis, Part 2. Microbiological and Biochemical Properties* (eds Weaver RW, Angle JS, Bottomly PJ), pp. 256–267. Soil Science Society of America, Madison, WI.

Vieten B, Blunier T, Neftel A, Alewell C, Conen F (2007) Fractionation factors for stable isotopes of N and O during N_2O reduction in soil depend on reaction rate constant. *Rapid Communications in Mass Spectrometry*, **21**, 846–850.

Vieten B, Conen F, Neftel A, Alewell C (2009) Respiration of nitrous oxide in suboxic soil. *European Journal of Soil Science*, **60**, 332–337.

Weier KL, Doran JW, Power JF, Walters DT (1993) Denitrification and the dinitrogen nitrous-oxide ratio as affected by soil-water, available carbon, and nitrate. *Soil Science Society of America Journal*, **57**, 66–72.

Zar JH (1998) *Biostatistical Analysis* (4th edn). Prentice Hall, Upper Saddle River, NJ, USA.

Supporting Information

Additional Supporting Information may be found in the online version of this article:

Figure S1. Surface flux chamber headspace concentrations of $^{15}N_2O$ (closed circles) and SF_6 (open circles) over the measurement period at Plot 30 in March 2009.

Data S1. References.

Table S1. Published fractionation factors associated with N_2O production via nitrification.

Table S2. Published fractionation factors associated with N_2O production via denitrification.

Table S3. Published fractionation factors associated with N_2O reduction to N_2.

Please note: Wiley-Blackwell are not responsible for the content or functionality of any supporting materials supplied by the authors. Any queries (other than missing material) should be directed to the corresponding author for the article.

Author Query Form

Journal: GCB
Article: 2481

Dear Author,
During the copy-editing of your paper, the following queries arose. Please respond to these by marking up your proofs with the necessary changes/additions. Please write your answers on the query sheet if there is insufficient space on the page proofs. Please write clearly and follow the conventions shown on the attached corrections sheet. If returning the proof by fax do not write too close to the paper's edge. Please remember that illegible mark-ups may delay publication.
Many thanks for your assistance.

Query reference	Query	Remarks
1	AUTHOR: Punshon et al. 2004 has been changed to Punshon and Moore, 2004 so that this citation matches the Reference List. Please confirm that this is correct.	
2	AUTHOR: Millington and Quick (1961) has been changed to Millington and Quirk (1961) so that this citation matches the Reference List. Please confirm that this is correct.	
3	AUTHOR: Please give manufacturer information for all products: company name, town, state (if USA), and country wherever applicable.	
4	AUTHOR: The meaning of 'SF_6 and $^{15}N_2O$ concentrations' is incomplete, please check.	
5	AUTHOR: Please provide all editors with initials for Prather et al. (1995).	

MARKED PROOF

Please correct and return this set

Please use the proof correction marks shown below for all alterations and corrections. If you wish to return your proof by fax you should ensure that all amendments are written clearly in dark ink and are made well within the page margins.

Instruction to printer	*Textual mark*	*Marginal mark*
Leave unchanged	··· under matter to remain	New matter followed by ⌐ or ⌐(x2)
Insert in text the matter indicated in the margin	⌐	
Delete	/ through single character, rule or underline or ⊢⊣ through all characters to be deleted	⌐/ or ⌐/(x2)
Substitute character or substitute part of one or more word(s)	/ through letter or ⊢⊣ through characters	new character / or new characters /
Change to italics	— under matter to be changed	⌐
Change to capitals	≡ under matter to be changed	≡
Change to small capitals	= under matter to be changed	=
Change to bold type	~ under matter to be changed	~
Change to bold italic	≈ under matter to be changed	≈
Change to lower case	Encircle matter to be changed	≠
Change italic to upright type	(As above)	⌐
Change bold to non-bold type	(As above)	⌐
Insert 'superior' character	/ through character or ⌐ where required	Y or Y under character e.g. Y^{3} or Y^{3}
Insert 'inferior' character	(As above)	⌐ over character e.g. Y_{2}
Insert full stop	(As above)	⊙
Insert comma	(As above)	,
Insert single quotation marks	(As above)	Y or Y and/or Y or Y
Insert double quotation marks	(As above)	Y or Y and/or Y or Y
Insert hyphen	(As above)	⊢
Start new paragraph	⌐	⌐
No new paragraph	⌐	⌐
Transpose	⌐	⌐
Close up	linking ⁀ characters	⁀
Insert or substitute space between characters or words	/ through character or ⌐ where required	Y
Reduce space between characters or words	| between characters or words affected	⊤